ISSN 2079-0864, Biology Bulletin Reviews, 2016, Vol. 6, No. 5, pp. 365–385. © Pleiades Publishing, Ltd., 2016.
Original Russian Text © D.O. Logofet, N.G. Ulanova, I.N. Belova, 2015, published in Zhurnal Obshchei Biologii, 2015, Vol. 76, No. 6, pp. 438–460.

Polyvariant Ontogeny in Woodreeds: Novel Models and New Discoveries

D. O. Logofet[a], *, N. G. Ulanova[b], **, and I. N. Belova[a]

[a] *Obukhov Institute of Atmospheric Physics, Russian Academy of Sciences, per. Pyzhevskii 3, Moscow, 119017 Russia*

[b] *Moscow State University, Moscow, 119234 Russia*

**e-mail: danilal@postman.ru*

***e-mail: nulanova@mail.ru*

Received March 16, 2015

Abstract—Polyvariant ontogeny (PVO) gets a visual expression in the life cycle graphs (LCGs) for *Calamagrostis* woodreeds as a *variety of pathways* for individual plants to develop through many of their states, which are distinguishable by the ontogenetic stage and chronological age (in years). PVO is recognized as the basic mechanism of adaptation in local populations of grasses to their environments, while a quantitative measure of adaptation is found by constructing a matrix model for the double-structured population, calibrating its matrix of vital rates from empirical data, and calculating the dominant eigenvalue λ_1. This approach encounters an obstacle typical for grasses: while the rates of aging and ontogenetic transitions can be determined from field data mainly by the morphology of aboveground parts of the plant, the rates of vegetative propagation can be reliably determined only from digging up the belowground rhizome system, i.e., by destroying the sample plot ("reproductive uncertainty"). Therefore, the former (nondestructive) calibrations of matrix models were, to an extent, subjective, resulting in correspondingly subjective estimations. A novel method to overcome the reproductive uncertainty makes use of the *maximization hypothesis*: the uncertain rates are such that λ_1 attains its maximal possible value under the given conditions. To test the hypothesis, we have conducted a field study by a new technique with a model species, the woodreed *Calamagrostis epigeios* (L.) Roth, which vegetatively reproduces in a meadow phytocenosis and a spruce forest clearance. Excavating the whole system of ramets with their rhizomes and analyzing the parent–offspring links in laboratory, we have gained (in addition to the former data on the local population structures and ontogenetic transitions) a new kind of data to calculate the status-specific rates of reproduction. The novel calibration method has enabled us to find an exact range of λ_1 values, i.e., the true quantitative bounds of adaptation for a given local population. Obtained under the reproductive uncertainty and maximality hypothesis, the values of λ_1 have turned out to be close to the upper bounds of the ranges, thus verifying the hypothesis. The study has discovered some generative subsidiary plants that sprout from the rhizomes of maternal ramets without entering the virginal stage. As a result, the LCG is enriched with new reproductive pathways, and there are new (not yet published) situations, in which λ_1 fails in its accuracy as a measuring tool of comparative plant demography. We propose a general method to adjust the adaptation measure in this kind of situation.

DOI: 10.1134/S2079086416050042

The concept of polyvariant development as the variety of ontogenetic pathways appeared in plant physiology (Sabinin, 1963) to be later adopted in geobotany. The polyvariant ontogeny is a manifestation of the variation retained by individuals of a local population over ontogeny or during its individual stages. Our research is concentrated on the study of *dynamic* (temporal) polyvariance, which, according to the classification by Zhukova (1986, 1995), comprises the diversity of individual developmental rates and the duration of individual ontogenetic stages. A few studies of this polyvariance commenced after the 1990s (Zhukova and Komarov, 1990); however, this type of polyvariance remains the least studied according to Akshentsev (Akshentsev et al., 2006). The main attention is focused on the sequence and duration of ontogenetic stages in long-term monitoring of the labeled individuals on permanent plots in natural cenopopulations and plantings of a species (Onipchenko and Komarov, 1997; Ermakova et al., 2001; Ulanova et al., 2002). However, most studies are reduced to the mere construction of developmental schemes according to the ontogenetic stages for some species.

Polyvariant ontogeny (PVO) is considered the major mechanism underlying the adaptation to varying environmental conditions in a local plant population. However, the question of a quantitative measure for this adaptation remains open. To solve this problem, an original technique for the construction of matrix models for the single-species population dynamics of perennial plants with complex (*polyvariant*) life cycles has been elaborated in earlier projects on the population dynamics of local *Calamagrostis* woodreeds (Ulanova et al., 2002, 2008; Logofet,

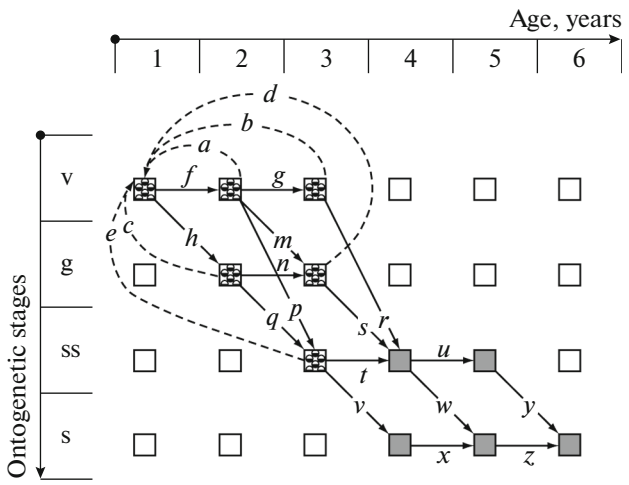

Fig. 1. LCG for the *C. canescens* woodreed as a sample of polyvariant ontogeny in an age-stage-structured population. Stages: **v**, *virginal*; **g**, *generative*; **ss**, *subsenile*; and **s**, *senile*; the fleeting stages of *plantule, juvenile*, and *immature* plant are included into the one-year virginal stage. The empty small squares represent the imaginary (unobserved) age-stage states; the patterned squares are the states involved in reproduction; solid arrows correspond to aging and ontogenetic transitions for 1 year; the dashed arrows indicate vegetative reproduction; Latin letters denote the status-specific rates of transitions or reproduction (adapted from Ulanova et al., 2002).

2002). The technique is based on the idea of population structure (developed in the national school of geobotany) as a set of age-stage groups of plants; note that the developmental stage of an individual plant by the moment of observation is determined according to the so-called "scales of age states" in the species under study (Uranov, 1967, 1975; Rabotnov, 1978; Zaugol'naya et al., 1988; Ulanova, 2000, 2006; etc.), while the chronological age (years) is assessed by an original technique (Ulanova, 2006). Correspondingly, the state of a model population at time t is described by the *vector of population structure*, $x(t)$, the components of which are the (absolute) numbers of the corresponding age-stage groups recorded at that moment on permanent sample plots in nature. Tracking the labeled individuals (*partial ramets*) over two or more years enables us to determine the ages at which the ontogenetic stages are realized in a species under study and the transitions which are possible between stages in one year. This gives rise to a formal description of the plant life cycle as a *life cycle graph* (LCG), which is defined on a finite two-dimensional integer-valued "lattice" of statuses (Fig. 1) and reflects the variety of ontogenetic and plant reproduction trajectories under the given conditions. Multiple ontogeny variants appear due to alternative transitions (*arcs*[1] from states $\mathbf{v}^1$, $\mathbf{v}^2$, $\mathbf{g}^2$, $\mathbf{ss}^3$, and $\mathbf{ss}^4$, where the superscript denotes the plant age (years). This reflects the biotic potential of the ruderal species (i.e., its population ability to grow fast and propagate), and LCG provides a conceptual basis for constructing a corresponding matrix model that describes the observed double-structure population dynamics at the phase of unlimited extensive growth. While PVO is recognized as an adaptation mechanism at the level of species cenopopulation, the matrix model of this population gives a *quantitative measure* for its adaptation as the dominant eigenvalue, λ_1, of the corresponding matrix.

In a matrix model, the population state (or *structure*) is projected one time step forward (1 year in our case) according to the following equation:

$$\boldsymbol{x}(t+1) = \boldsymbol{L}\boldsymbol{x}(t), \tag{1}$$

where matrix $\boldsymbol{L}$, referred to as *projection matrix* (Caswell, 1989, 2001), is (element-wise) *nonnegative* and formally corresponds to the given LCG as the matrix associated with a given directed graph (*ibid.*; Logofet and Belova, 2008).

The projection matrix is traditionally represented as the sum of two matrices, $\boldsymbol{L} = \boldsymbol{T} + \boldsymbol{F}$, where matrix $\boldsymbol{T}$ contains only the elements responsible for aging and ontogenetic transitions (*transition matrix*) and matrix $\boldsymbol{F}$ has only the *reproduction rates* for structural groups (*fertility matrix;* Cushing and Yicang, 1994; Caswell, 2001; Li and Schneider, 2002); the remaining elements of $\boldsymbol{T}$ and $\boldsymbol{F}$ matrices are zero.

The results of the matrix model become quantitatively certain only after the projection matrix has been *calibrated* from the experimental data. The earlier projects on *Calamagrostis* local populations gained data of the type referred to as "identified individuals with uncertain parents" (Logofet, 2010, 2013b, 2013c; Logofet et al., 2012). The individuals are "identified" (Caswell, 2001) since the annual labeling and census of all ramets on the permanent sample plot (Ulanova and Demidova, 2001; Ulanova et al., 2002, 2008; Logofet et al., 2006) made it possible to reliably determine the vectors $\boldsymbol{x}(t)$ for several successive time moments $t = 0, 1, 2, \ldots$. Moreover, the recorded changes in the status of each plant from each status group j ($j = 1, 2, \ldots, n$) since the previous year, for example, since the time $t = 0$, made it possible to count the number of plants N_{ij} with status j that changed their status at the next time moment for i ($i = 1, 2, \ldots, n$). According to model (1), this number is $\tau_{ij}x_j(0)$, where τ_{ij} is an element (i, j) of the transition matrix $\boldsymbol{T}$ (the share of individuals with status j that changes it for status i) 1 year later. Hence, each element of the matrix was calculated uniquely as

$$\tau_{ij} = \begin{cases} N_{ij}/x_j(0), & \text{if } x_j(0) \neq 0, \\ 0, & \text{if } x_j(0) = 0, \end{cases} \tag{2}$$

quantifying matrix $\boldsymbol{T}$ into a pattern conforming to the LCG (Fig. 1).

[1] The directed links of the graph are referred to as *arcs* even if they are shown as straight segments.

The virginal ramets without labels represented the population recruitment over the previous year, which according to the first equation in system (1) is

$$x_1(1) - \tau_{11}x_1(0) = f_p x_p(0) + \ldots + f_r x_r(0), \qquad (3)$$

where p and r are the numbers of the first (sequentially in vector $\boldsymbol{x}$) and the last reproductive status groups and $f_p, f_{p+1}, \ldots, f_r$ are nonzero elements in the first row of matrix $\boldsymbol{F}$ (f_j is the average number of offspring per one parent plant of status j to be found next year in status $\mathbf{v}^1$; Logofet, 2013b, 2013c, 2013d). The data prevented determination of the parental ramets for the recruiting ones i.e., the contributions of individual reproductive groups to summation (3) remain principally uncertain ("reproductive uncertainty," ibid.); thus, calibration of the matrix $\boldsymbol{L} = \boldsymbol{T} + \boldsymbol{F}$ required additional conditions/assumptions.

Different ways to cope with reproductive uncertainty can be found in the literature (Logofet, 2008); however, they contradict the biology of the species and do not respond the idea of PVO as an adaptation mechanism. Svirezhev's substitution principle (Logofet, 2010) implies that uncertainty in data can be replaced with an "empirical generalization," which is a statement that is free of the shortcomings mentioned above and imposes an additional condition sufficient to solve the problem. In our case, such generalization is the *maximization hypothesis:* the distribution of contributions to overall recruitment is such that the value of potential population growth, or the adaptation measure $\lambda_1(\boldsymbol{L})$, is maximal under the given population structure (*ibid.*) Thus, the calibration problem reduces to a (nonlinear) problem to maximize the λ_1 under (linear) constraints ensuing from the field data. It was shown (Logofet, 2013a, 2013b) that a solution of the problem does exist and is unique in practical situations, i.e., the maximization hypothesis actually removed the reproductive uncertainty and made it possible to obtain a more objective estimate for adaptation measure as a tool for comparative studies.

However, the maximization hypothesis did not fit theoretical views of some researchers on the absence of optimality in the course of biological evolution (Metz et al., 2008a, 2008b; Gyllenberg and Service, 2011) and required empirical verification.

Here, we propose a new technique for a field experiment targeted at verification of the maximization hypothesis in the framework of a matrix population model for the age-stage-structured population of *C. epigeios* (L.) Roth. woodreed. For this purpose, the experiment is designed so that not only the transition matrix $\boldsymbol{T}$ but also the fertility part $\boldsymbol{F}$ of the projection matrix $\boldsymbol{L} = \boldsymbol{T} + \boldsymbol{F}$ is directly computable from the field data through restoration of the complete picture of mother–offspring links in a colony of ramets on the sample plots laid in different habitats. This, along with the quantitative assessment and comparison of different local populations according to their adaptation measure $\lambda_1(\boldsymbol{L})$, makes it possible to compare the computed $\lambda_1(\boldsymbol{L})$ to the measure $\lambda_1(\boldsymbol{L}_{\text{run}})$, which is derived from the part of the experimental data that meets the terms of reproductive uncertainty under the maximization hypothesis for each of the local populations. Such a comparison has been performed for cenopopulations in a meadow habitat and on a spruce forest felling; the conclusion is that the maximization hypothesis is true in its refined formulation.

The new field-experiment technique has also revealed a new, previously undescribed phenomenon in the woodreed PVO: besides forming the 1-year virginal offspring, the maternal rhizomes of generative ramets also produce offspring at a generative stage. The two-stage recruitment leads to a specific feature in the LCG structure that has never been noticed in the literature on matrix models. This specific feature results in an inaccuracy in λ_1 as a measuring tool of comparative demography, and we propose a way to remove the inaccuracy in such cases.

MATERIALS AND METHODS

Objects. *C. epigeios* is a herbaceous perennial polycarpic long-rhizome grass. An adult plant consists of many uneven-aged, rosette, polycyclic intravaginal, and extravaginal shoots forming a system of partial tufts, a colony (Ulanova, 1995; Ulanova et al., 2008). The *C. epigeios* woodreed has di- and polycyclic shoots with a well-defined multinodal rosette shoot and a few-nodal culm with pronounced akrotony. There are no elongated vegetative shoots (Serebryakova, 1971).

The vegetative mobility is caused by an increase in the plagiotropic shoots (rhizomes) acting as vegetative renewal organs. Senile particulation of the colony does not occur as the rhizomes do not rot with age, retaining the connection of all ramets in the colony. Dried tufts remain at rhizomes, but the rhizome continues to function as a conducting system (Bel'kov, 1960).

The biology of this species is well studied, making it a good model species for solving several experimental problems. The population structure of the model woodreed species has been studied during extensive population growth with vegetative spreading in open plant communities without any competition with other species. The age-stage structure of a typical growing population with a complete ontogenetic cycle in the selected plots reflected their adaptation state in the examined felling and meadow phytocenoses.

The studies were conducted in a meadow in the Moscow River floodplain and a felling of spruce forest in quadrant 1 and the eastern part of quadrant 7 of the Zvenigorod Biological Station of the Moscow State University (Odintsovo district, Moscow oblast), respectively. Studied were plots dominated completely by the woodreed, where patches of 3- and 4-year-old plants prevailed.

The meadow 1 and meadow 2 plots reside in a *C. epigeios* woodreed meadow formed on abandoned arable land in a high floodplain area 4 years ago. The soils are alluvial, humus–gley (meadow), rich in mineral nutrients. Meadow grasses (*Dactylis glomerata* and *Bromopsis inermis*), *Taraxacum officinale,* and *Lysimachia nummularia* grew up in the herbage at low abundances. The felling 3 and felling 4 plots were laid on a clear-cut overgrowth in a spruce forest. The soils are soddy-podzolic with a dense sod horizon formed by woodreed shoots and rhizomes. Shrubs of *Frangula alnus* Mill., *Sorbus aucuparia* L., and *Salix caprea* L. have grown up in the woodreed biocenosis. Under the canopy of woodreed, *Fragaria vesca* L., *Convallaria majalis* L., *Rubus saxatilis* L., *Asarum europaeum* L., *Vaccinium myrtillus* L., and *Luzula pilosa* (L.) Scop. are growing. The two selected phytocenoses differ not only in their origin, but also in the set of ecological conditions. The meadow habitat conditions are better for the woodreed; its generative shoots are stronger and their height there reaches 1.2–1.5 m versus 0.9–1.2 m in the felling habitat.

Methods. Plots with an area of 1×1 m^2 were laid in mid-August (when the woodreed tuft development was completed) in sites with complete woodreed prevalence. The plots were dug to a depth of 20–30 cm, starting from the boundaries of the southwestern corner, to release gradually soil layers and the overall woodreed rhizome system. Gradually dusting the soil from rhizomes, all of the systems of partial tufts (ramets) were piled into bags. The tufts were disassembled and analyzed in the laboratory.

The morphology and ramet structure of *C. epigeios* woodreed were well studied earlier (Ulanova, 1995); thus, the chronological age of individual grass can be determined from the structure of annual growth in its tillering zone and the developmental stage of each ramet from the known "scale of ontogeny" (Ulanova et al., 2007). All the alive woodreed tufts and those that died in 2014 in each plot were dug out, preserving the rhizome system connecting them with alive daughter tufts of all generations. This enabled us to determine the maternal-offspring hierarchy of the ramets, date the year at which the offspring ramets were formed, and assess the developmental stage of the parent ramet in the previous year according to the ratio of dry vegetative and generative shoots of the ramet (Fig. 2[2]). Each ramet was given its age-stage characteristics at the moment of excavation (August 2014), and its status in the previous year was restored. Also the alive daughter rhizomes were counted (see Table 1 for a fragment of the primary data), which served for direct calculation of the actual contribution of each age-stage group to the population recruitment due to vegetative propagation in each of the four plots. Hereinafter, the superscript in the designation of a status group denotes the plant age (years), and the subscript shows the category within the ontogenetic stage. The characteristic of category $\mathbf{v}_2$ is a larger ramet size as compared with $\mathbf{v}_1$, as well as the development of two or more living vegetative shoots (Ulanova, 2006); however, they were united into one stage, **v**, in further calculations, because this is more frequently used in plant population biology (Zaugol'nova et al., 1988). The ramets with generative shoots were divided into three categories according to the common practice (as in the earlier projects), namely, $\mathbf{g}_1$, young generative; $\mathbf{g}_2$, middle-aged; and $\mathbf{g}_3$, old generative (Ulanova et al., 2007, 2008; Logofet et al., 2011).

Further ramet counting according to status groups gave the quantitative cenopopulation structure at the time of excavation, $\boldsymbol{x}$ (2014); to restore the structure of $\boldsymbol{x}$ (2013), all ramets that died in the previous year were taken into account. Considering the changes in status over all of the ramets within the plot, we obtained a complete picture of the transitions in the given plot over 1 year, i.e., the transition part of LCG, to get N_{ij} values and transition rates according to Eq. (2).

Statistical characteristics (mean and variance for the daughter rhizomes per one parental ramet) were calculated for each phytocenosis.

To complete the construction of LCG with its reproductive part, for each ramet of cenopopulation recruitment (each row in Table 1 where the 2013 status cell is blank), we determined its maternal plant by the rhizome link and lined up a general survival scheme of young rhizomes from the parents in different status groups (Fig. 3).

Quantitatively analyzing the summary tables of characteristics for the vegetative and generative spheres, including the tillering node, and counting the number of daughter rhizomes for all ramets, we revealed a certain regular pattern: the daughter rhizomes were always more abundant than the ramets that formed in spring because some rhizomes died in winter. We cannot always specify the mortality pattern of those rhizomes in detail when digging them out. A high ramet density in the examined plots (400–800 per 1 m^2) sometimes prevents the retention of the links between maternal and daughter ramets. The parental ramet gives rise to several daughter rhizomes, and the new ramets developing from these rhizomes may be at both the virginal ($\mathbf{v}^1$) and generative ($\mathbf{g}_1^1$ or $\mathbf{g}_2^1$) stages.

The content of Fig. 3 allows the construction of plot-specific LCGs to be completed in their reproductive part; however, the quantitative ratio of the daughter ramets at different stages cannot be determined if part of the rhizomes is torn during excavation. In such cases, the status of the parental plant remains uncertain, and a mathematical task arises to find the exact numbers a, b, c, ..., g, and h; Figs. 3a–3d) of daughter ramets from the rhizomes of the parents in each status, i.e., the task to determine the contribution of each

[2] Figure by O.V. Cherednichenko.

Fig. 2. Fragment of the *C. epigeios* woodreed colony (the system of partial ramets): (*1*) maternal rhizome; (*2*) final rhizomes; (*3*) new growing rhizomes; (*4*) virginal 1-year-old ramet, $\mathbf{v}^1$; (*5*) virginal 2-year-old ramet, $\mathbf{v}^2$; (*6*) generative 3-year-old ramet, $\mathbf{g}_1^3$; and (*7*) dry 4-year-old ramet (Logofet et al, 2014, under permission).

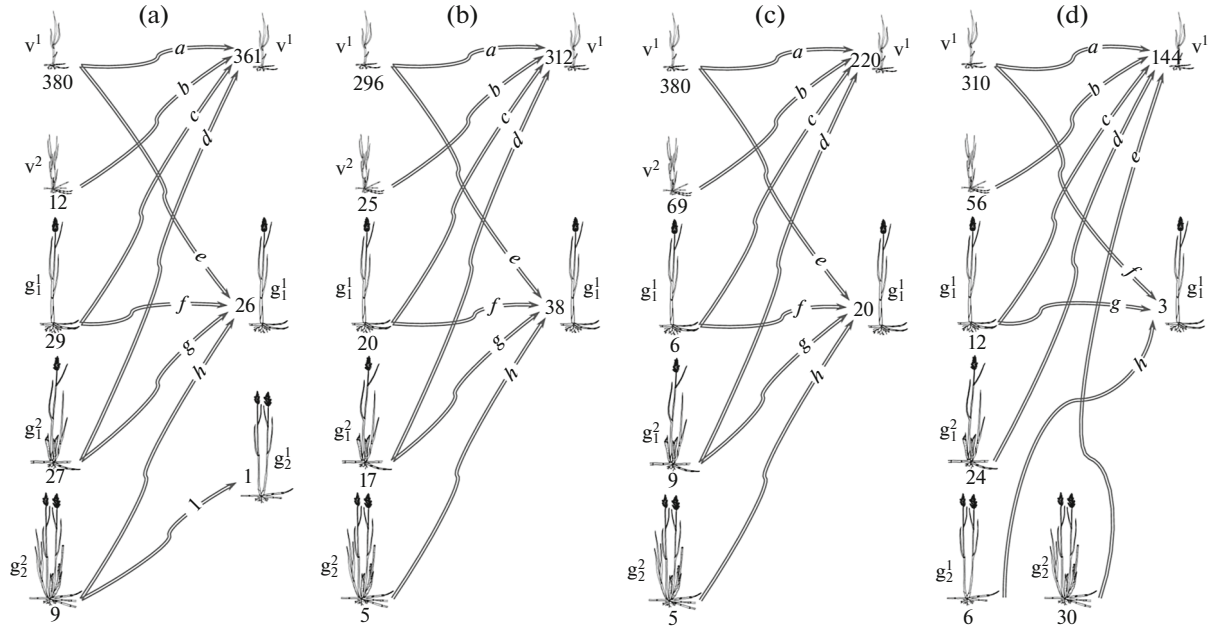

Fig. 3. Survival schemes for young rhizomes of various parental groups. The total number of young rhizomes developed from the parents of the corresponding status is shown below the image of parental ramet; *a*, *b*, *c*, …, *g*, and *h* denote the number of living daughter ramets for the parents of the corresponding status. Variants by the results of excavating the plots: (a) meadow 1; (b) meadow 2; (c) felling 3; and (d) felling 4.

age-stage-specific group to the status-specific recruitment of the population. The solution to this problem is nontraditional (see below) and allows the precise bounds for an adaptation measure of a given cenopopulation to be determined based on the data gained.

The range of λ_1 values for each plot. The equations and inequalities relating parameters *a*, *b*, ... , *g*, and *h* with the outcome of analyzing the belowground part of the colony ensue from the constructed survival schemes for daughter rhizomes. In particular, the fol-

Table 1. Fragment of the summary table with biomorphological description of woodreed plants in the meadow 2 plot

Ramet no.	2014				2013			
	status	the umber of			status	the number of		
		vegetative shoots	generative shoots	daughter rhizomes		vegetative shoots	generative shoots	daughter rhizomes
1	$\mathbf{v}_1^1$	1		1				0
2	$\mathbf{v}_1^1$	1		1				0
3	$\mathbf{v}_1^1$	1		1				0
4	$\mathbf{ss}^3$	1		1	$\mathbf{g}_1^2$	1		2
5	$\mathbf{v}_1^2$	1		1	$\mathbf{v}_1^1$	1		1
6	$\mathbf{v}_1^1$	1		2				0
7	$\mathbf{g}_1^1$	1		0				0
8	$\mathbf{g}_1^2$		1	1	$\mathbf{v}_2^1$	2	1	1
9	$\mathbf{v}_1^1$	1		1				0
10	$\mathbf{v}_1^1$	1		1				0
11	$\mathbf{ss}^2$	1		0	$\mathbf{v}_1^1$	1		1
12	$\mathbf{v}_1^1$	1		0				0
13	$\mathbf{v}_1^1$	1		0				0
14	$\mathbf{ss}^2$	1		0	$\mathbf{v}_1^1$	1		3
15	$\mathbf{v}_1^1$	1		1				0
16	$\mathbf{v}_1^1$	1		1				0
17	$\mathbf{g}_1^1$	1	1	1			1	0
18	$\mathbf{g}_1^2$	1	1	0	$\mathbf{v}_2^1$	2	1	1
19	$\mathbf{v}_1^1$	1		2				0
20	$\mathbf{v}_1^1$	1		2				0
21	$\mathbf{v}_1^1$	1		2				0
22	$\mathbf{v}_1^1$	1		0				0

lowing system of two equations and five inequalities ensue from Fig. 3b for the meadow 2 plot:

$$\begin{cases} a+b+c+d=312, \\ e+f+g+h=28, \\ a+e\le 296,\ b\ge 25,\ c+f\le 20,\ d+g\le 17,\ h\le 5, \end{cases} \quad (4)$$

where the unknowns can take on nonnegative integer values only. The analogous system for the felling 3 plot (Fig. 3c) is

$$\begin{cases} a+b+c+d=220, \\ e+f+g+h=20, \\ a+e\le 240,\ b\ge 69,\ c+f\le 6,\ d+g\le 9,\ h\le 5. \end{cases} \quad (5)$$

Equations for the unknowns taking only integer values are called *Diophantine equations* (*Akedemik,* 2000; Bashmakova, 2007). According to traditional concepts (formed by the theory of systems of linear algebraic equations), a system can have a unique solution when the number of equations coincides with the number of unknowns. The number of equations in Diophantine systems is substantially less (as in our case), but the integer values and other constraints allow the combinatorial number of solution variants to be drastically reduced.

An additional constraint emerged from an expert idea of the quantitative hierarchy among the shares $S(\mathbf{s})$ of the daughter rhizomes developed from the par-

ents with different **s** statuses that gave offspring, namely,

$$S(\mathbf{v}^1) \geq S(\mathbf{g}_1^1) \geq S(\mathbf{v}^2) \geq S(\mathbf{g}_1^2) \geq S(\mathbf{g}_2^2). \quad (6)$$

We also took into account any significant bounds from below provided by the daughter ramets of unambiguously identified parents. The solutions were found by an algorithm iterating through all possible variants.

For each of the finite number of solutions to the Diophantine system with constraints (6), we further formed the projection matrix $\boldsymbol{L}$ (in accordance with the constructed LCG) of the matrix population model, i.e., system of equations (1), where $\boldsymbol{x}$ ($t = 2013$) and $\boldsymbol{x}(2014)$ are the vectors of age-stage structure restored from the excavation data in each of the plots. For each matrix $\boldsymbol{L}$, its dominant eigenvalue $\lambda_1(\boldsymbol{L}) > 0$ was calculated as the *measure of adaptation* of cenopopulation with the observed set of status-specific reproduction rates, an analog of the traditional (Fisher's) fitness for multidimensional population (Logofet et al., 2006, 2014; Logofet, 2013a). The maximum and maximum $\lambda_1(\boldsymbol{L})$ were found among the (finite number of) the obtained values to get the range $[\lambda_{1\min}, \lambda_{1\max}]$ as a tool for comparing the local populations in the quantitative measure of adaptation

RESULTS

Cenopopulation structures. The technique implemented to analyze the dug woodreed colony allowed us to determine the cenopopulation structures in 2014 and restore those structures for 2013 (Table 2). These structures are characteristic of all four plots; the $\mathbf{v^1}$ ramets are prevalent (accounting for 46–74% of all ramets), while $\mathbf{v^2}$ ramets (6–29%) and all generative (**g**) ramets (5–19%) are less abundant. The meadow plots house a few **ss** ramets (5–10%); only some of them reach the age of 4 years. The woodreed ontogeny under favorable meadow conditions is faster, with a few ramets senescing, while the majority perishes at adult stages not reaching the **ss** and **s** stages. The felling habitat displays another pattern: a considerable share of the ramets (9–18%) ends its life cycles at **ss** and **s** stages, with many ramets reaching the age of 4 years.

Along with the restoration of cenopopulation structures, the analysis of the relations between the belowground and aboveground parts of the colony has revealed certain survival statistics for the newly formed ramets in different phytocenoses (Table 3). The mean values and variances for the number of rhizomes in the felling and a meadow differ in a statistically significant manner: 99% according to t-test ($t > t_{0.01}$) and Fisher's test ($F > F_{0.01}$), respectively.

LCGs and the limits to cenopopulation fitness. The LCGs corresponding to the obtained structures and rhizome link patterns (Figs. 3a–d) are shown in Fig. 4 and illustrate the polyvariance of PVO itself even within a single habitat. Every LCG unambiguously (accurate to the numbering of components in population structure vectors) determines projection matrix $\boldsymbol{L}$, which depends on parameters a, b, ..., g, and h, while each solution to Diophantine system (5)–(6) and analogous systems gives quantitative certainty to $\boldsymbol{L}$, enabling us to calculate $\lambda_1(\boldsymbol{L})$. The results of these calculations are listed in Table 4.

The minimal possible λ_1 values are considerably larger than unity for all plots except felling 4, where still $\lambda_{1\max} > 1$. These results quantitatively confirm the expert opinion on extensive growth in young populations, the growth rate in the meadow being greater than that in the felling habitat (the growth almost ceased in the felling 4 plot, where $\lambda_{1\max} > 1$ by only 0.03). The absolute width ($\lambda_{1\max} - \lambda_{1\min}$) of the fitness measure range varies from 0.0425 in the meadow 2 plot to 0.2269 in the felling 3 plot or from 2.8 to 17.6% ($100(\lambda_{1\max} - \lambda_{1\min})/\lambda_{1\max}$). On the whole, the second and third plots have ranges $[\lambda_{1\min}, \lambda_{1\max}]$ located more to the right on the real axis than the first and fourth, respectively, indicating a difference in growth conditions even within a single habitat.

Testing the maximal adaptation hypothesis. The obtained data on the cenopopulation structures allow for calibration of the $\boldsymbol{L}$ matrices ($\boldsymbol{L} = \boldsymbol{T} + \boldsymbol{F}$), where $\boldsymbol{T}$ is calculated according to (2) directly from the data, while the search of F is based on the maximization hypothesis, i.e., without using the data on direct counting of status-specific reproduction rates (elements of $\boldsymbol{F}$). As is mentioned above, the calibration problem then reduces to a nonlinear maximization problem for $\lambda_1(\boldsymbol{L})$ with the linear constraints stemming from the data. Here, the unknown variables are no longer the absolute numbers (a, b, ..., h) of the daughter ramets developed from parental plants of different statuses, but rather the proportional elements ($r_a, r_b, ..., r_h$) of matrix $\boldsymbol{F}$, i.e., the mean (per one parental individual of a particular status) numbers of alive offspring at a certain stage. Equality constraints are the analogs of equation (3): the component-wise equations of system (1) that describe the recruitment of population via the elements of F and the structure vectors $\boldsymbol{x}(t)$ (Table 2). The constructed LCGs (Fig. 4) suggest that two such equalities hold for each plot (Table 4; Appendix A).

The situation with inequality constraints is more complex. Although the hierarchy of conditions (6) can be equivalently expressed in terms of parameters r_a, r_b, ..., r_h, the denominators in the respective inequalities are known only from the "belowground" analysis. Coarsening these inequalities leads to a *heuristic hierarchy*, the very simple form (A2) of which no longer depends on the details of the belowground sphere.

A special role is played in posing the maximization problem by *bounds*, which are grouped as a special class of constraints in the Matlab syntax (Appendix A),

Table 2. Age-stage structure of *C. epigeios* in 2013 and 2014 in four studied pots

Stages	2013, ramet age (years)				Total number of ramets	2014, ramet age (years)				Total number of ramets
	1	2	3	4		1	2	3	4	
Meadow 1										
v	294	24	2			361	81	0		
$\mathbf{g_1}$	25	29				26	67			
$\mathbf{g_2}$	0	10	0			1	8	2		
$\mathbf{g_3}$		02					2	7		
ss		2	10	0	398		10	16	4	585
Vector	[294, 24, 2, 25, 29, 0, 10, 0, 0, 2, 2, 10, 0]^T					[361, 81, 0, 26, 67, 1, 8, 2, 2, 7, 10, 16, 4]^T				
Meadow 2										
v	218	27	1			312	78	0		
$\mathbf{g_1}$	13	18	2			28	16	0		
$\mathbf{g_2}$		5	0				0	1		
$\mathbf{g_3}$			0					3		
ss		6	19	7	316		10	11	2	461
Vector	[218, 27, 1, 13, 18, 2, 5, 0, 0, 6, 19, 7]^T					[312, 78, 0, 28, 16, 0, 0, 1, 3, 10, 11, 2]^T				
Felling 3										
v	303	81	5			220	124	6		
$\mathbf{g_1}$	4	15	0			20	39	1		
$\mathbf{g_2}$		2					7			
$\mathbf{g_3}$		1	2				1	6		
ss		4	47	8			15	30	9	
s			20	16	508			2	3	483
Vector	[303, 81, 5, 4, 15, 0, 2, 1, 2, 4, 47, 8, 20, 16]^T					[220, 124, 6, 20, 39, 1, 7, 1, 6, 15, 30, 9, 2, 3]^T				
Felling 4										
v	193	37	2			144	82	6		
$\mathbf{g_1}$	7	11				3	2			
$\mathbf{g_2}$	2	14	1			0	1	0		
$\mathbf{g_3}$		1	4				2	0		
ss		7	8	0			11	15	3	
s		2	9	2	300		3	4	5	281
Vector	[193, 37, 2, 7, 11, 2, 14, 1, 1, 4, 7, 8, 0, 2, 9, 2]^T					[144, 82, 6, 3, 2, 0, 1, 0, 2, 0, 11, 15, 3, 3, 4, 5]^T				

Blank cells indicate that no ramets of the corresponding age-stage status have been detected after excavating the plot. The vector is obtained by concatenating the table structure by rows.

the constraints being semantically important to test the hypothesis.

Equalities (3) themselves cause the parameters to be already bounded from *above;* however, rejection of the positive *lower bounds* brings to zero values of some parameters in the formal solution to the optimization problem, which contradicts the presence of the corresponding reproductive arcs in the LCGs. If the constraint maximization problem is solved (as in our case) after analysis of the belowground part of the colony and solution of the Diophantine system of equations and inequalities (Table 4), then the values (A4) close to actually observed ones will be the best choice of the *lower* and *upper* bounds. The corresponding solution λ_1^* is the closest to the range $[\lambda_{1\min}, \lambda_{1\max}]$ of its true values and coincides in the integer parameters $[a, b, \ldots, h] = \boldsymbol{p}$ with most components of the vector $\boldsymbol{p}$ for $\lambda_{1\max}$ (Table 4; Appendix A).

Since the calibration according to λ_1 maximization is intended to replace the laborious belowground analysis, we need the *a priori* bounds to formulate the problem, i.e., the bounds that are specified in the absence (or without taking into account) the results obtained by analyzing the rhizome links. The variant (A4) described above is not of an *a priori* nature in this sense and is used in this project to illustrate and check the algorithm of constraint maximization. However, if we omit the details in the belowground sphere structure and use the experimental statistical data summarized over the phytocenoses in the average number of young rhizomes per parent plant (Table 3), this value, for example, for meadow, is 1.329 ± 0.762, whereby the averaged lower bound for the reproductive rate equals 0.567. However, this *uniform statistical* bound turns out to be in conflict with one of the equality constraints (Appendix A), and the constrained maximization problem has no solution.

A practically efficient choice of the a priori bounds for reproduction parameters is based on the following consideration. Since the formal optimization often reaches the parameter boundary values, the uniform and/or too coarse bounds give a solution that, while the best in formal optimality, noticeably distorts the actual pattern of reproduction. That is why the a priori bounds should not be uniform as above; they should rather be chozen as a function of the status of the maternal ramets. For example, it is possible to fit the *heuristic hierarchy* of inequalities a priori embedded into the constraint maximization problem (Appendix A, conditions (A2) and (A5)).

It is logical that many of the optimal parameter values a^*, b^*, ..., h^* (recalculated from r^*) turn out to be integers, despite posing the maximization problem in real numbers, i.e., over the more powerful set of feasible values. However, when noninteger values are optimal, they logically improve the solution optimality, i.e., elevate the λ_1^* value (although not greater than the third decimal place) as compared with the corresponding set of integer values. Thus, the values $\lambda_1^* > \lambda_{1\max}$ found by the maximization principle localize close to the range of true λ_1 values (Table 4; Appendix A). Therefore, the maximization hypothesis is confirmed in its refined formulation: when found as the maximum possible value under the observed constraints, the λ_1 value is the closer to the actual range of values, the more accurate bounds are given in the constraint maximization problem for the status-specific reproduction rates.

Reproductive core of LCGs and the "off-core" reproductions. The Perron–Frobenius theorem for nonnegative matrices, the mathematical foundation of matrix population models, applies primarily to *irreducible matrices* (Gantmacher, 1966), while the criterion of irreducibility reduces to the *strong connectedness* of the digraph associated with a given matrix

Table 3. Number of young rhizomes that formed woodreed ramets in 2014

Statistical values	Meadow	Felling
Sample size	747	663
Mean*	1.329	1.525
t-Test	4.373	
$t_{0.01}$-Test	2.576	
Deviation, σ	0.762	0.848
Variance, σ^2	0.581	0.718
Fisher's test, F	1.238	
$F_{0.01}$ test	1.000	

* Per one parental ramet.

(Harary et al., 1965; Horn and Johnson, 1990; Logofet, 1993), i.e., of the LCG in our case. If a population structure contains postreproductive groups, the corresponding matrix $\boldsymbol{L}$ turns out to be *reducible,* while the LCG is not strongly connected. This means that the dominant eigenvalue $\lambda_1(\boldsymbol{L})$ of matrix $\boldsymbol{L}$ is actually the λ_1 of its irreducible principal submatrix associated with the *reproductive core* (Logofet, 2008, 2013a), the maximal strongly connected subgraph of the LCG comprising the reproductive arcs (the reproductive cores in Fig. 4 are marked with gray background). In turn, this means that the reproduction rates that correspond to the LCG arcs outgoing from (or/and ingoing to) the vertices outside the reproductive core have no effect on the value of $\lambda_1(\boldsymbol{L})$. These are the following arcs: $\mathbf{g}_2^2 \to \mathbf{g}_2^1$ in Fig. 4a, $\mathbf{g}_2^2 \to \mathbf{g}_2^1$ in Fig. 4b, and $\mathbf{g}_2^1 \to \mathbf{g}_1^1$ in Fig. 4d.

These off-core reproductive arcs create a contradictory situation. On the one hand, they contribute, to a low but still nonzero degree, to population reproduction and growth, although these contributions are omitted in the $\lambda_1(\boldsymbol{L})$ value, the measure of fitness for a given cenopopulation. On the other hand, the presence of the off-core reproductions means a higher degree of PVO as compared with their absence, hence such a cenopopulation should formally have a higher fitness too. The general meaning of the off-core reproductive arcs consists in a certain acceleration of the reproduction process, which implies a higher fitness. Since the $\lambda_1(\boldsymbol{L})$ measure is exactly the same in the absence of the off-core reproductive arcs in LCGs, the described situation reveals inaccuracy of $\lambda_1(\boldsymbol{L})$ as a measuring tool to compare cenopopulations in their degree of fitness. We can eliminate this inaccuracy by reasoning in analogy to that for the experiment of 2013 (Logofet et al., 2014).

Let $\mu(\boldsymbol{L}) \geq \lambda_1(\boldsymbol{L})$ denote an accurate measure of cenopopulation fitness; note that $\mu(\boldsymbol{L}) > \lambda_1(\boldsymbol{L})$ when the LCG has off-core reproductive arcs. Consider the LCG for an imaginary (virtual) population where all

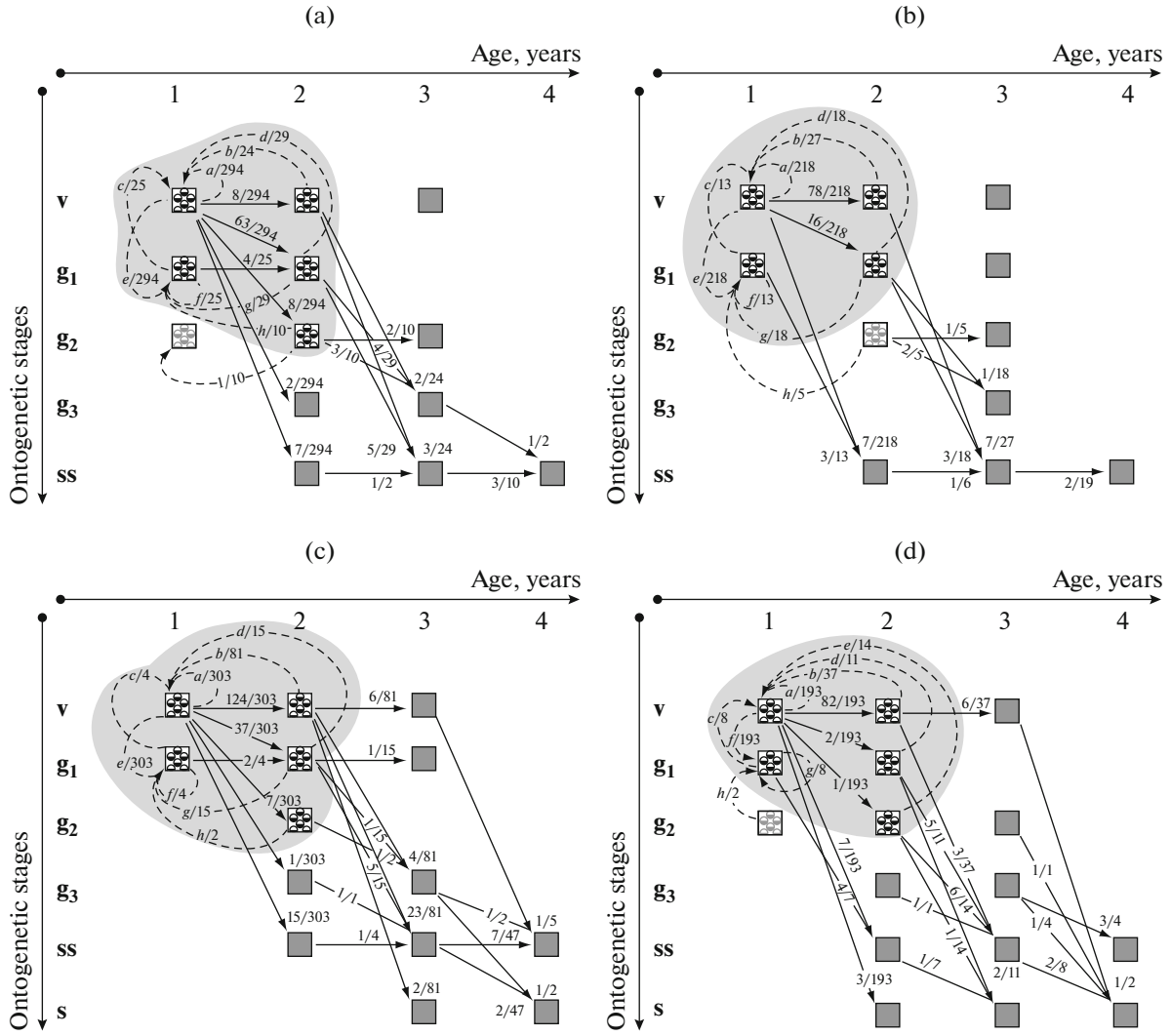

Fig. 4. LCG for the *C. epigeios* woodreed by the outcome of excavating the plots with 4-year-old plants in 2014 (after the immature and virginal stages having been aggregated into a single stage, **v**). See Fig. 3 for the meaning of parameters *a*, *b*, …, *g*, and *h*. Gray denotes the LCG *reproductive core* (see text for explanations).

the off-core reproductive arcs are redirected and included into the core, for example, arc $\mathbf{g}_2^2 \to \mathbf{g}_2^1$ is replaced with $\mathbf{g}_2^2 \to \mathbf{g}_1^1$ (Fig. 4a), an outgoing status of arc $\mathbf{g}_2^2 \to \mathbf{g}_2^1$ (Fig. 4b) is replaced with $\mathbf{g}_1^2$, and an outgoing status of arc $\mathbf{g}_2^1 \to \mathbf{g}_1^1$ (Fig. 4d) is replaced with $\mathbf{g}_1^1$. As a result, the new $\boldsymbol{L}_{\text{vir}}$ matrix is obtained from the original $\boldsymbol{L}$ matrix by increments in the corresponding elements. As a result, $\lambda_1(\boldsymbol{L}_{\text{vir}}) > \lambda_1(\boldsymbol{L})$, since the Frobenius eigenvalue of any irreducible matrix is a monotone increasing function of its elements (Gantmacher, 1966; Horn and Johnson, 1990). However, $\lambda_1(\boldsymbol{L}_{\text{vir}})$ is still less than $\mu(\boldsymbol{L})$ because the virtual population (all else being equal) now has no accelerating effects of the off-core reproductions from the real population. Thus,

$$\mu(\boldsymbol{L}) = \lambda_1(\boldsymbol{L}_{\text{vir}}) + \varepsilon(\boldsymbol{L}, \boldsymbol{L}_{\text{vir}}), \qquad (7)$$

where $\varepsilon(\boldsymbol{L}, \boldsymbol{L}_{\text{vir}})$ is a small positive variable relating the contributions of common and off-core reproductions to the fitness of cenopopulation and proportional to, for example, the matrix norm (Horn and Johnson, 1990, Section 5.6; Caswell, 2001, Section A.8) of the difference $\boldsymbol{L} - \boldsymbol{L}_{\text{vir}}$ (Logofet et al., 2014) with a coefficient of the order of magnitude as the difference $\lambda_1(\boldsymbol{L}_{\text{vir}}) - \lambda_1(\boldsymbol{L})$. See Appendix B for the corresponding calculations and Table 4 for results. The error of $\lambda_1(\boldsymbol{L})$ as compared with $\mu(\boldsymbol{L})$ has ranged in different plots from a few thousandths to hundredths of unity.

Table 4. Calculation of the numbers of living daughter ramets as the solutions of Diophantine systems of equations and inequalities and the corresponding ranges of $\lambda_1(\boldsymbol{L})$ values

Status of parental ramet in 2013	Status of parental ramet in 2013	Status of daughter ramet in 2014	Additional constraints (6) and the reliable ones from below	Matrix $\boldsymbol{L}$ and its reproductive-core submatrix	Values of a, ..., h for λ_{1min}	Values of a, ..., h for λ_{1max}
Meadow 1 $a+b+c+d=361$, $e+f+g+h=26$					$\lambda_{1min}=$ 1.2594	$\lambda_{1max}=$ 1.3182
$\mathbf{v}^1$	a	$\mathbf{v}^1$	$(a+e)/380 \geq (c+f)/29$	$a/294$ $b/24$ 0 $c/25$ $d/29$ 0 0 | 0 0 0 0 0 0	354	325
$\mathbf{v}^2$	b	$\mathbf{v}^1$	$b/12 \geq (d+g)/27$	81/294 0 0 0 0	5	10
$\mathbf{g}_1^1$	c	$\mathbf{v}^1$	$(c+f)/29 \geq b/12$	$e/294$ 0 0 $f/25$ $g/29$ 0 $h/10$ | 0 0 0 0 0 0	1	7
$\mathbf{g}_1^2$	d	$\mathbf{v}^1$	$(d+g)/27 \geq (h+1)/9$	63/294 0 0 4/25 0 0 0 0 0 0 1/10 | 0 0 0 0 0 0	1	19
$\mathbf{v}^1$	e	$\mathbf{g}_1^1$	$e \geq 3$	8/294 0 0 0 0 0 0 0 0 0 2/10 0	4	3
$\mathbf{g}_1^1$	f	$\mathbf{g}_1^1$	$f \geq 6$	2/294 0 0 0 0 0 0 0 0 2/24 0 0 0 4/29 0 3/10 0 0 0	12	18
$\mathbf{g}_1^2$	g	$\mathbf{g}_1^1$	$g \geq 3$	7/294 0 0 0 0 0 0 0 0 0 3/24 0 0 5/29 0 0 0 0 0 1/2 0	8	3
$\mathbf{g}_2^2$	h	$\mathbf{g}_1^1$	$h \geq 2$	0 0 0 0 0 0 0 0 1/2 0 3/10 0	2	2
			Number of solutions: 38928	Refined measure (7), $\mu(\boldsymbol{L})$:	1.2596	1.3193

Table 4. (Contd.)

Status of parental ramet in 2013	Status of parental ramet in 2013	Status of daughter ramet in 2014	Additional constraints (6) and the reliable ones from below	Matrix $\boldsymbol{L}$ and its reproductive-core submatrix	Values of a, ..., h for $\lambda_{1\min}$	Values of a, ..., h for $\lambda_{1\max}$
Meadow 2					$\lambda_{1\min}$ = 1.4945	$\lambda_{1\max}$ = 1.5370
$a+b+c+d=312$, $e+f+g+h=28$						
$\mathbf{v}^1$	a	$\mathbf{v}$	$(a+e)/296 \geq (c+f)/20$	$\begin{bmatrix} a/218 & b/27 & 0 & c/13 & d/18 & 0 & 0 & 0 & 0 & 0 & 0 & 0 \\ 78/218 & 0 & & & & & & & & & & \\ 0 & 0 & 0 & & & & & & & & & \\ e/218 & 0 & 0 & f/13 & g/18 & 0 & h/5 & 0 & 0 & 0 & 0 & 0 \\ 16/218 & 0 & 0 & 0 & 0 & & & & & & & \\ 0 & 0 & 0 & 0 & 0 & 0 & & & & & & \\ 0 & 0 & 0 & 0 & 0 & 0 & & & & & & \\ 0 & 0 & 0 & 0 & 0 & 1/5 & 0 & & & & & \\ 0 & 0 & 0 & 1/18 & 0 & 2/5 & 0 & 0 & & & & \\ 7/128 & 0 & 0 & 3/13 & 0 & 0 & 0 & 0 & 0 & & & \\ 0 & 7/27 & 0 & 0 & 3/18 & 0 & 0 & 0 & 1/6 & 0 & & \\ 0 & 0 & 0 & 0 & 0 & 0 & 0 & 0 & 0 & 2/19 & 0 & \end{bmatrix}$	289	271
$\mathbf{v}^2$	b	$\mathbf{v}^1$	$b/25 \geq (d+g)/17$		15	23
$\mathbf{g}_1^1$	c	$\mathbf{v}^1$	$(c+f)/20 \geq b/25$, $c \geq 2$		2	16
$\mathbf{g}_1^2$	d	$\mathbf{v}^1$	$(d+g)/17 \geq h/5$, $d \geq 2$		6	2
$\mathbf{v}^1$	e	$\mathbf{g}_1^1$	$e \geq 3$		7	18
$\mathbf{g}_1^1$	f	$\mathbf{g}_1^1$	$f \geq 3$		15	3
$\mathbf{g}_1^2$	g	$\mathbf{g}_1^1$	$g \geq 4$		4	5
$\mathbf{g}_2^2$	h	$\mathbf{g}_1^1$	$h \geq 2$		2	2
			Number of solutions: 16850	Refined measure (7), $\mu(\boldsymbol{L})$:	1.5420	1.5916

Table 4. (Contd.)

Status of parental ramet in 2013	Status of parental ramet in 2013	Status of daughter ramet in 2014	Additional constraints (6) and the reliable ones from below	Matrix $\boldsymbol{L}$ and its reproductive-core submatrix	Values of $a, \ldots, h$ for $\lambda_{1\min}$	Values of $a, \ldots, h$ for $\lambda_{1\max}$
Felling 3					$\lambda_{1\min} =$ 1.0623	$\lambda_{1\max} =$ 1.2892
$a + b + c + d = 220$, $e + f + g + h = 20$						
$\mathbf{v^1}$	a	$\mathbf{v^1}$	$a \geq 136$*	$\begin{bmatrix} a/303 & b/81 & 0 & c/4 & d/15 & 0 & 0 & 0 & 0 & 0 & 0 & 0 & 0 & 0 \\ 124/303 & 0 & & & & & & & & & & & & \\ 0 & 6/81 & 0 & & & & & & & & & & & \\ & & & & & & & & & & & & & \\ e/303 & 0 & & f/4 & g/15 & 0 & h/2 & & & & & & & \\ 37/303 & 0 & 0 & 2/4 & 0 & & & & & & & & & \\ 0 & 0 & 0 & 0 & 1/15 & 0 & & & & & & & & \\ 7/303 & 0 & 0 & 0 & 0 & 0 & 0 & & & & & & & \\ 1/303 & 0 & 0 & 0 & 0 & 0 & 0 & 0 & & & & & & \\ 0 & 4/18 & 0 & 0 & 1/15 & 0 & 1/2 & 0 & 0 & & & & & \\ 15/303 & 0 & 0 & 0 & 0 & 0 & 0 & 0 & 0 & 0 & & & & \\ 0 & 23/81 & 0 & 0 & 5/15 & 0 & 0 & 1/1 & 0 & 1/4 & 0 & & & \\ 0 & 0 & 1/5 & 0 & 0 & 0 & 0 & 0 & 1/2 & 0 & 7/47 & 0 & & \\ 0 & 2/81 & 0 & 0 & 0 & 0 & 0 & 0 & 0 & 0 & 0 & 0 & 0 & \\ 0 & 0 & 0 & 0 & 0 & 0 & 0 & 0 & 1/2 & 0 & 2/47 & 0 & 0 & 0 \end{bmatrix}$	170	147
$\mathbf{v^2}$	b	$\mathbf{v^1}$	$b/69 \geq (d + g)/9$		46	69
$\mathbf{g_1^1}$	c	$\mathbf{v^1}$	$(c + f)/6 \geq b/69$, $c \geq 2$		2	2
$\mathbf{g_1^2}$	d	$\mathbf{v^1}$	$(d + g)/9 \geq h/5$, $d \geq 2$		2	2
$\mathbf{v^1}$	e	$\mathbf{g_1^1}$	$e \geq 3$		11	4
$\mathbf{g_1^1}$	f	$\mathbf{g_1^1}$	$f \geq 3$		3	4
$\mathbf{g_1^2}$	g	$\mathbf{g_1^1}$	$g \geq 4$		4	7
$\mathbf{g_2^2}$	h	$\mathbf{g_1^1}$	$h \geq 2$		2	5
			Number of solutions: 440	Refined measure (7), $\mu(\boldsymbol{L})$:	$= \lambda_1(\boldsymbol{L})$	

Table 4. (Contd.)

Status of parental ramet in 2013	Status of parental ramet in 2013	Status of daughter ramet in 2014	Additional constraints (6) and the reliable ones from below	Matrix $\boldsymbol{L}$ and its reproductive-core submatrix	Values of $a, \ldots, h$ for $\lambda_{1\min}$	Values of $a, \ldots, h$ for $\lambda_{1\max}$
Felling 4					$\lambda_{1\min} =$ 0.8834	$\lambda_{1\max} =$ 1.0331
$a+b+c+d=144$, $e+f+g+h=36$						
$\mathbf{v}^1$	a	$\mathbf{v}^1$	$(a+f)/310 \geq (c+g)/12$	$a/193$ $b/37$ 0 $c/8$ $d/11$ 0 $e/14$ 0 0 0 0 0 0 0 0 0	77	78
				82/193 0		
$\mathbf{v}^2$	b	$\mathbf{v}^1$	$b/56 \geq d/24$	0 6/37 0	36	56
				$f/193$ 0 0 $g/11$ $h/2$ 0 0 0 0 0 0 0 0 0 0		
$\mathbf{g}_1^1$	c	$\mathbf{v}^1$	$b \geq 36$*	2/193 0 0 0 0	2	2
				0 0 0 0 0 0		
$\mathbf{g}_1^2$	d	$\mathbf{v}^1$	$d/24 \geq h/6$, $d \geq 3$	1/193 0 0 0 0 0 0	4	4
				0 0 0 0 0 0 0 0		
$\mathbf{g}_2^2$	e	$\mathbf{v}^1$	$e \geq 4$	0 0 0 0 0 0 0 0 0	25	4
				0 0 0 0 0 0 0 0 0 0		
$\mathbf{v}^1$	f	$\mathbf{g}_1^1$	$f \geq 1$	7/193 0 0 4/7 0 0 0 0 0 0 0	1	1
				0 3/37 0 0 5/11 0 6/14 0 1/1 0 0 0		
$\mathbf{g}_1^1$	g	$\mathbf{g}_1^1$	$g \geq 1$	0 0 0 0 0 0 0 0 0 3/4 0 0 0	1	1
				3/193 0 0 0 0 0 0 0 0 0 0 0 0 0		
$\mathbf{g}_2^1$	h	$\mathbf{g}_1^1$	$h \geq 1$	0 0 0 0 2/11 0 1/14 0 0 0 1/7 0 0 0 0	1	1
				0 0 1/2 0 0 0 0 1/1 0 1/4 0 2/8 0 0 0 0		
			Number of solutions: 2022	Refined measure (7), $\mu(\boldsymbol{L})$:	0.9309	1.0734

* Refined hierarchy (6).

DISCUSSION

The woodreed population biology attracts the particular interest of researchers since the species of this genus (especially *C. epigeios*) are regarded as the most aggressive and dominating the early stages of succession, and they actively colonize free areas in Europe (Prach and Pysek, 1999). The ecology of *C. epigeios* is unique since this species grows under almost any moisture conditions and soil richness; in its life strategy, this is a typical ruderal species. As a strong edificator, the woodreed holds the territory in the meadow and young felling areas for many years and significantly alters the environment both in the aboveground and belowground spheres (Ulanova, 1995).

The *major* life cycle of *C. epigeios* woodreed (i.e., of the plants germinated from *seeds*) proceeds with strengthening the shoots of sequential orders (Serebryakova, 1971); the principal axis and shoots develop but do not pass the complete developmental cycle, being smaller and weaker than the subsequent-order shoots. Only the third-order shoots can complete the full cycle of development. All the shoots are di- or polycyclic and are of the fourth-year flowering (*ibid.*).

Here, we consider the *minor* life cycle, namely, the tufts developing from the apical buds of rhizomes. Patrabolova (1953) described in detail the formation and development of a partial tuft from the rhizome. The apical buds of rhizomes, curving upwards, give rise to the principal axis of partial tufts. The formation of lateral shoots begins on the axis during the first year in the life of a tuft, when the axis is represented by a growing bud (immature stage), and continues during the second year, when the principal axis is a shortened rosette shoot (virginal stage). The principal axis of partial ramets begins flowering in the third year of their life (young generative stage); then the ramet persists for 1–2 years more with the last of its lateral shoots, which may (middle-aged and old generative stage) or may not flower (subsenile and senile stages) and then completely dies. Patrabolova (1953) studied the woodreed ontogeny in the pine plantings of the Buzuluk pine forest (steppe zone). Our studies in young spruce fellings of the Tver oblast (southern taiga zone, Central Forest State Nature Biosphere Reserve) also confirm that the ramets flower in the third year of their lives; note that the flowering is typical of the ramets of the third and second generations (Ulanova, 1995, 1996). According to our data, the *C. epigeios* woodreed can flower even in the second year in favorable environments.

Janczyk-Weglarska (1997) observed the *C. epigeios* PVO in Poland under natural conditions of the broadleaved forests. The woodreed in a pine forest has a reduced ontogeny without flowering, a complete ontogeny with flowering in the third–fourth years in fellings, and a complete ontogeny with flowering only in the third year with transition to senile stage in the fourth year in alluvial soils and meadows. The author experimentally demonstrated (ibid.) that PVO (in particular, the development of the monocarpic shoots within a single plant) do not represent a genetically controlled trait but is phenotypically determined by habitat conditions, i.e., it represents rather a *modification* (phenotypic) variation of an adaptive nature under specific growth conditions.

Previous studies of woodreed ontogenies revealed the need to rejuvenate (to enter the virginal stage) for the daughter ramets formed on the rhizomes of parent plants at the generative stage. Our study has discovered generative daughter ramets growing on the rhizomes of generative parent plants that did not pass rejuvenation but flowered in the first year of ramet formation. Acceleration of the shoot growth rate acquires a special significance under the conditions maximally favorable for the development of the young colonies with extensive growth and without competition with other species. Presumably, the coniferous-deciduous forest zone is favorable for the woodreed growth, along with the fact that no droughts and cold periods occurred in the spring–summer season of 2014. These are comfortable environments for woodreed development which seem to create the conditions for the uniquely rapid development of the generative shoots.

Our discovery is formally expressed in the fact that the LCG contains more than one *recruiting stage* (Protasov and Logofet, 2014; Fig. 4), i.e., the stage of population increase, unlike the LCGs described in the previous projects (Fig. 1). This fact complicates the model mathematics: the matrix $\boldsymbol{L} = \boldsymbol{T} + \boldsymbol{F}$ can no longer be considered a *rank-one correction* (*ibid.*) of the transition matrix $\boldsymbol{T}$ since the rank of the corresponding matrix $\boldsymbol{F}$ is 2; hence, the theorem (*ibid.*) on the indicator ability of function $R_1(\boldsymbol{L}) = 1 - \det(\boldsymbol{I} - \boldsymbol{L})$ is no longer applicable. However, the technical advantages of *indication* (Logofet, 2012) are lost not for this reason but because $R_1(\boldsymbol{L})$ as a function of the reproductive parameters $a, b, \ldots, g$ and h loses the property to be linear, which is inherent in rank-one corrections. However, the *indicator ability* does preserve: the calculations demonstrate that $R_1(\boldsymbol{L}) > 1$ in all the cases in Table 4 where $\lambda_1 > 1$ and that $R_1(\boldsymbol{L}) < 1$ when $\lambda_1 < 1$. This observation raises a question on whether the theorem on rank-one corrections (or rather, its consequences for the matrices $\boldsymbol{L}$; Protasov and Logofet, 2014) can be expanded in what concerns the indicator ability of function $R_1(\boldsymbol{L})$.

The presence of more than one recruiting stage is not unique for discrete-structured populations (Werner and Caswell, 1977; Shea and Kelly, 1998; Weppler et al., 2006; Pathikonda et al., 2009); the uniqueness of our LCGs is of another kind: three of the four graphs (Figs. 4a, 4b, and 4d) contain reproductive arcs beyond the reproductive core (we named them the off-core arcs). Some authors neglected the need to deter-

mine the reproductive core in the LCG and the corresponding principal submatrix when calculating the dominant eigenvalue (Logofet, 2013d and the references therein), which may lead to erroneous overestimation of the λ_1 value (*ibid.*). However, the fact that λ_1 is inaccurate when the "core rule" is met and when an off-core arc is present has been noticed only in the paper describing the results of our 2013 study (Logofet et al., 2014). Meanwhile, the effects of ontogeny acceleration mentioned above require the adaptation measure, $\mu(\boldsymbol{L})$, to be also augmented for such cenopopulations above the inaccurate $\lambda_1(\boldsymbol{L})$ value; only when the arcs of "accelerated" generative plants remain within the reproductive core (Fig. 4c), the former measure retains its accuracy: $\mu(\boldsymbol{L}) = \lambda_1(\boldsymbol{L})$ (Table 4).

Note that the presence/absence of *transition arcs* from the corresponding states (or to the corresponding states) is crucial for the presence/absence of off-core reproductive arcs in LCGs: for example, the absence of $\mathbf{g}_2^1 \to \mathbf{g}_2^2$ arc (Figs. 4a and 4d) and the presence of $\mathbf{v}^1 \to \mathbf{g}_2^2$ arc (Fig. 4c). This fact is certainly detectable from the examination of the aboveground part of the colony alone (i.e., under conditions of reproductive uncertainty), while the presence of accelerating reproductive arcs themselves can be just postulated, as is actually done above (section "Testing the maximal adaptation hypothesis"), when we used the LCGs constructed from the excavation data (Fig. 4).

To calculate the dominant eigenvalue, $\lambda_1(\boldsymbol{L})$, under the reproductive uncertainty and the maximization hypothesis means to solve the constraint maximization problem for reproduction rates under the known equality constraints and a priori bounds (Logofet, 2010, 2013b, 2013c). A specific feature of this study is that we complement the problem with the inequality constraints reflecting the expert idea of the hierarchy among the contributions by various status groups to the annual population recruitment (Appendix A). At a first glance, the hierarchy is completely a "belowground" knowledge (Table 4; parameters *a*, *b*, ..., *g*, and *h*), and it is inappropriate to recommend it as a practice for the "aboveground" calibration. However, since the belowground parameters are proportional to the reproduction rates $\boldsymbol{r}_a$, $\boldsymbol{r}_b$, ..., and $\boldsymbol{r}_h$ to be optimized (with a proportion coefficient known from the data on population structure, $\boldsymbol{x}$(2013), Table 2), the actual hierarchy, (6), can in fact be converted to an a priori *heuristic* one (A2) to be included into the maximization problem.

As regards the a priori bounds for this problem, it is easy to choose them when the data for belowground sphere are in hand, and it is no wonder that maximization in this case gives the same result (Appendix A, column (A4)) as the counting of daughter ramets (Table 4). Unfortunately, the bounds are no longer "a priori" in this case. In other words, the intimate mechanism concealed under the ground that forms the aboveground reproduction rates does not allow the a priori bounds to be sufficiently fine. On the other hand, even the preliminary results of the field experiment (Logofet et al., 2014) demonstrate that the maximal adaptation hypothesis is true to the degree to which the chosen bounds are status-specific (Logofet, 2013b) and close to the results of analysis of the belowground part of the colony. That is why a priori bounds (A5) fit for heuristic hierarchy (A4) turned out a reasonable way out of the deadlock, while the results gained on verifying the maximization hypothesis (Appendix A) allowed the formulation of the hypothesis to be improved.

CONCLUSIONS

The concept of PVO as an adaptation mechanism of local populations gets a vivid illustration in the LCGs of woodreed age-stage-structured populations, while the corresponding matrix models provide a quantitative measure of adaptation as the dominant eigenvalue λ_1 of the projection matrix. Matrix calibration according to aboveground censuses faces the challenge of reproductive uncertainty since the rhizome links of the recruitment ramets with the parent ones are hidden in the soil. The challenge was answered by the adoption of the maximal adaptation hypothesis, and the field study to test it has been performed by a new technique with the *C. epigeios* woodreed vegetatively propagating in a meadow habitat and a spruce forest felling. Excavation of the sample plots and analysis of the system of partial ramets linked by rhizomes have revealed a new phenomenon in the ontogeny of woodreed when it grows vegetatively, namely, the 1-year-old ramets originating from generative parents and recruiting the population at the generative stage, in addition to those at the virginal stage. These findings have also predetermined a new calibration method, namely, counting directly the status-specific rates of reproduction in a combinatorial number of variants to eliminate the residual uncertainty. Thereby, we have established the reliable ranges of values for the measure of fitness in the excavated local populations.

The λ_1 values mined from part of the data under the maximization hypothesis turned out close to the upper bound of the range, while an updated statement of the λ_1 constraint maximization problem and the ensuing solution confirmed the hypothesis in a revised formulation. The field experiment motivated by the need for reliable calibration of the model matrix, has also revealed situations that are novel for matrix models, in which λ_1 loses its accuracy as the measure for adaptation and requires an adequate refinement as a tool for comparative demography.

APPENDIX A

Calibrating Projection Matrices under the Hypothesis of Maximality

The method for calibrating matrix $\boldsymbol{L}$ under the reproductive uncertainty of the data (Logofet, 2012, 2013b, 2013c) from the meadow 1 plot according to LCG (Fig. 4a) and structure vectors $\boldsymbol{x}(2013)$ and $\boldsymbol{x}(2014)$ (Table 2) makes use of the same *equality constraints* as those in the Diophantine system (Table 4), but the unknown parameters here are the elements of matrix $\boldsymbol{F}$ arranged in the vector $\boldsymbol{r} = [r_a, r_b, ..., r_h]^T$:

$$294r_a + 24r_b + 25r_c + 29r_d = 361, \quad (A1)$$
$$294r_e + 25r_f + 24r_g + 10r_h = 26,$$

or in the vector-matrix form $\boldsymbol{A}_{eq}\boldsymbol{r} = \boldsymbol{B}_{eq}$:

$$\begin{bmatrix} 294 & 24 & 25 & 29 & 0 & 0 & 0 & 0 \\ 0 & 0 & 0 & 0 & 294 & 25 & 29 & 10 \end{bmatrix} \begin{bmatrix} r_a \\ r_b \\ r_c \\ r_c \\ r_c \\ r_f \\ r_g \\ r_h \end{bmatrix} = \begin{bmatrix} 361 \\ 26 \end{bmatrix}. \quad (A1')$$

If the hierarchy of *inequality constraints* (6) is put down using parameters $\boldsymbol{r}$, we obtainm

$$294(r_a + r_c)/380 \geq 25(r_c + r_f)/29 \geq 24\, r_b/12$$
$$\geq 29(r_d + r_g)/27 \geq 10(r_h + 1)/9,$$

where the denominator numbers are not really known under the terms of reproductive uncertainty. In this system of inequalities, all coefficients are close to unity except for the coefficient for r_b, which is 2. Correspondingly, the *heuristic* analogs for conditions (6) in the a priori setting of maximization problem take on the form

$$(r_a + r_e) \geq (r_c + r_f) \geq 2r_b \geq (r_d + r_g) \geq r_h, \quad (A2)$$

or in the vector-matrix form $\boldsymbol{A}\boldsymbol{r} \leq \boldsymbol{B}$:

$$\begin{bmatrix} -1 & 0 & 1 & 0 & -1 & 1 & 0 & 0 \\ 0 & 2 & -1 & 0 & 0 & -1 & 0 & 0 \\ 0 & -2 & 0 & 1 & 0 & 0 & 1 & 0 \\ 0 & 0 & 0 & -1 & 0 & 0 & -1 & 1 \end{bmatrix} \begin{bmatrix} r_a \\ r_b \\ r_c \\ r_c \\ r_c \\ r_f \\ r_g \\ r_h \end{bmatrix} \leq \begin{bmatrix} 0 \\ 0 \\ 0 \\ 0 \end{bmatrix}. \quad (A2')$$

Equalities (A1) impose certain upper bounds on the parameters, and the best choice of the lower and upper bounds, i.e., of the vectors $\boldsymbol{r}_{low}, \boldsymbol{r}_{up} > \boldsymbol{0}$, such that the conditions

$$\boldsymbol{r}_{low} \leq \boldsymbol{r} \leq \boldsymbol{r}_{up}, \quad (A3)$$

hold (component-wise) true, is provided by the vectors

$$\boldsymbol{r}_{low} = \min(\boldsymbol{r}_{min}, \boldsymbol{r}_{max}), \boldsymbol{r}_{up} = \max(\boldsymbol{r}_{min}, \boldsymbol{r}_{max}). \quad (A4)$$

Here $\boldsymbol{r}_{min}$ and $\boldsymbol{r}_{max}$ are the vectors recalculated from the obtained values of $a, ..., h$ (the penultimate and last columns of Table. 4, respectively), while the extreme values of two vectors are obtained in a component-wise manner. The *a priori* bounds fitting heuristic hierarchy (A2) are, for example,

$$(0.9 + 0.02) \geq (0.2 + 0.6) \geq 2*0.3$$
$$\geq (0.4 + 0.1) \geq 0.1 \text{ lower and}$$
$$(1.5 + 0.2) \geq (0.3 + 0.8) \geq 2*0.5$$
$$\geq (0.7 + 0.2) \geq 0.2 \text{ upper,}$$

i.e.,

$$\begin{aligned} \boldsymbol{r}_{low} &= [0.9\ 0.3\ 0.2\ 0.4\ 0.02\ 0.6\ 0.1\ 0.1]^T, \\ \boldsymbol{r}_{up} &= [1.5\ 0.5\ 0.3\ 0.7\ 0.2\ 0.8\ 0.2\ 0.2]^T. \end{aligned} \quad (A5)$$

Whether a particular choice of the bounds turns out to be feasible is also verified by its compatibility with equality constraint (A1), i.e., by holding the conditions $\boldsymbol{A}_{eq}\boldsymbol{r}_{low} \leq \boldsymbol{B}_{eq}$ and $\boldsymbol{A}_{eq}\boldsymbol{r}_{up} \geq \boldsymbol{B}_{eq}$.

Table 5 lists the *solutions* to the maximization problem, i.e., the vectors $\boldsymbol{r}^* = [r_a^*, r_b^*, \ldots r_h^*]^T$ meeting all conditions (A1)–(A3), and the corresponding values of $\lambda_1(\boldsymbol{L}^*) = \lambda_1^*$, obtained at the best (A4) and *heuristic* (A5) choices of the bounds by means of the Matlab function for constraint minimization, *fmincon* (MathWorks, 2012):

fmincon(@mlambda_N, $\boldsymbol{r}0$*,* $\boldsymbol{A}$*,* $\boldsymbol{B}$*,* $\boldsymbol{A}$eq*,* $\boldsymbol{B}$eq*,* $\boldsymbol{r}$low*,* $\boldsymbol{r}$up*).* (A6)

Here, *mlambda_N* is a user-defined function calculating the value of $(-\lambda_1)$ for the matrix $\boldsymbol{L}(\boldsymbol{r}) = \boldsymbol{T} + \boldsymbol{F}(\boldsymbol{r})$ from the input set $\boldsymbol{r}$ of the parameters (elements of $\boldsymbol{F}$) to be optimized and specific (according to $\boldsymbol{T}$ and the structure of $\boldsymbol{F}$) for each plot N; $\boldsymbol{r}_0$, the start point in searching for solution; and matrices $\boldsymbol{A}$, $\boldsymbol{B}$, ..., $\boldsymbol{r}$up are defined above.

Among the choices of lower bounds, the uniformly "statistical" one,

$$\boldsymbol{r}\text{low}^T = [0.5670, ..., 0.5670], \quad (A7)$$

was also considered. It gives $\boldsymbol{A}_{eq}\boldsymbol{r}_{low} = [211, 203]^T$ for the meadow 1 plot. Here $211 < 361$, which is permissible for the lower bounds, but $203 > 26$ is unfeasible under condition (A1'). Therefore, the problem had no solutions for this choice of the bound.

APPENDIX B

Reproductive Submatrices of Virtual Populations and the Refined Measures $\mu(\boldsymbol{L})$

Three of the four LCGs shown in Fig. 4 contain off-core reproductive arcs (Figs. 4a, 4b, and 4d). The

Table 5. Solutions (**r***) to the $\lambda_1(\boldsymbol{L})$ constraint maximization problem (A1)–(A3) with the status-specific bounds for the elements r_a, r_b, ... r_h of matrix $\boldsymbol{F}$ (from $\boldsymbol{L} = \boldsymbol{T} + \boldsymbol{F}$) to be optimized

Equality constraints (A1), $\boldsymbol{A}_{eq}$ $\boldsymbol{B}_{eq}$	Inequality constrains (A2), $\boldsymbol{A}$ $\boldsymbol{B}$	Parameters	Actual ($\boldsymbol{r}$*) and control (A4) solutions					
			$\boldsymbol{r}_{low}$	$\boldsymbol{r}$*	$\boldsymbol{r}_{up}$	(A4), $\boldsymbol{r}$	(A4), $\boldsymbol{p}$	$\boldsymbol{p}$
Meadow 1	$\begin{bmatrix}-1&0&1&0&-1&1&0&0\\0&2&-1&0&0&-1&0&0\\0&-2&0&1&0&0&1&0\\0&0&0&-1&0&0&-1&1\end{bmatrix}$	r_a	0.9	1.0946	1.5	1.1122	327.00	*a*
		r_b	0.3	0.4744	0.5	0.4167	10.00	*b*
$\begin{bmatrix}294&24&25&29&0&0&0&0\\0&0&0&0&294&25&29&10\end{bmatrix}$		r_c	0.2	0.3000	0.3	0.2000	5.00	*c*
		r_d	0.4	0.7000	0.7	0.6552	19.00	*d*
$\begin{bmatrix}361\\26\end{bmatrix}$	$\begin{bmatrix}0\\0\\0\\0\end{bmatrix}$	r_e	0.02	0.0200	0.2	0.0102	3.00	*e*
		r_f	0.6	0.6488	0.8	0.6333	15.83	*f*
		r_g	0.1	0.1000	0.2	0.1782	5.17	*g*
		r_h	0.1	0.1000	0.2	0.2000	2.00	*h*
$294r_a + 24r_b + 25r_c + 29r_d = 361$, $294r_c + 25r_f + 24r_g + 10r_h = 26$	$(r_a + r_c) \geq (r_c + r_f) \geq 2r_b \geq (r_d + r_g) \geq r_h$	λ_1^*		1.3280		1.3231	1.3231	λ_1
Meadow 2								
	$\begin{bmatrix}-1&0&\frac{1}{2}&0&-1&\frac{1}{2}&0&0\\0&1&-\frac{1}{2}&0&0&-\frac{1}{2}&0&0\\0&-1&0&1&0&0&1&0\\0&0&0&-1&0&0&-1&1\end{bmatrix}$	r_a	0.9	1.2376	1.5	1.2431	271.00	*a*
		r_b	0.6	0.9000	0.9	0.8519	23.00	*b*
$\begin{bmatrix}218&27&13&18&0&0&0&0\\0&0&0&0&218&13&18&5\end{bmatrix}$		r_c	0.4	1.1000	1.1	1.1385	14.80	*c*
		r_d	0.2	0.2000	0.4	0.1778	3.20	*d*
$\begin{bmatrix}312\\28\end{bmatrix}$	$\begin{bmatrix}0\\0\\0\\0\end{bmatrix}$	r_e	0.02	0.0417	0.2	0.0321	7.00	*e*
		r_f	0.8	1.1000	1.1	1.1538	15.00	*f*
		r_g	0.2	0.2000	0.4	0.2222	4.00	*g*
		r_h	0.2	0.2000	0.4	0.4000	2.00	*h*
$218r_a + 27r_b + 13r_c + 18r_d = 312$, $218r_c + 13r_f + 18r_g + 5r_h = 28$	$(r_a + r_c) \geq (r_c + r_f)/2 \geq r_b \geq (r_d + r_g) \geq r_h$	λ_1^*		1.5712		1.5643	1.5643	λ_1
Felling 3								
$\begin{bmatrix}303&81&4&15&0&0&0&0\\0&0&0&0&303&4&15&2\end{bmatrix}$	$\begin{bmatrix}0&3&-2&0&0&-2&0&0\\0&-3&0&2&0&0&2&0\\0&0&0&-2&0&0&-1&\frac{1}{2}\end{bmatrix}$	r_a	0.4	0.4663	1.0	0.4851	147.00	*a*
		r_b	0.8	1.0000	1.0	0.8519	69.00	*b*
		r_c	0.5	0.7000	0.7	0.5000	2.00	*c*
		r_d	0.1	0.2000	0.2	0.1333	2.00	*d*
$\begin{bmatrix}220\\20\end{bmatrix}$	$\begin{bmatrix}0\\0\\0\end{bmatrix}$	r_e	0.01	0.0116	0.2	0.0139	4.20	*e*
		r_f	0.7	1.0000	1.0	1.0000	4.00	*f*
		r_g	0.2	0.5000	0.5	0.4667	7.00	*g*
		r_h	1.0	2.5000	2.5	2.4000	4.80	*h*
$303r_a + 81r_b + 4r_c + 15r_d = 220$, $303r_c + 4r_f + 15r_g + 2r_h = 20$	$2(r_c + r_f) \geq 3r_b \geq 2(r_d + r_g) \geq r_h/2$	λ_1^*		1.3278		1.2884	1.2884	λ_1

Table 5. (Contd.)

Equality constraints (A1), A_{eq} B_{eq}	Inequality constrains (A2), A B	Parameters	Actual (r^*) and control (A4) solutions					
			r_{low}	r^*	r_{up}	(A4), r	(A4), p	p
Felling 4								
$\begin{bmatrix} 193 & 37 & 8 & 11 & 14 & 0 & 0 & 0 \\ 0 & 0 & 0 & 0 & 0 & 193 & 8 & 2 \end{bmatrix}$	$\begin{bmatrix} -1 & 0 & 1 & 0 & 0 & -1 & 1 & 0 \\ 0 & -1 & 0 & 1 & 0 & 0 & 0 & 0 \\ 0 & 0 & 0 & -1 & 0 & 0 & 0 & \frac{2}{3} \end{bmatrix}$	r_a	0.4	0.4187	1.0	0.4041	78.00	a
		r_b	0.8	1.5000	1.5	1.5135	56.00	b
		r_c	0.2	0.2000	0.7	0.2500	2.00	c
		r_d	0.3	0.3000	0.5	0.3636	4.00	d
$\begin{bmatrix} 144 \\ 3 \end{bmatrix}$	$\begin{bmatrix} 0 \\ 0 \\ 0 \end{bmatrix}$	r_e	0.2	0.2000	0.4	0.2857	4.00	e
		r_f	0.01	1.0104	0.2	0.0052	1.00	f
		r_g	0.1	0.1000	0.4	0.1250	1.00	g
		r_h	0.1	0.1000	0.6	0.5000	1.00	h
$193r_a + 37r_b + 8r_c + 11r_d + 14r_c = 144,\ 193r_f + 8r_g + 2r_h = 3$	$(r_a + r_f) \geq (r_c + r_g),\ r_b \geq r_d \geq 2r_h/3$	λ_1^*		1.0385		1.0331	1.0331	λ_1

Table 6. Reproductive-core submatrices L_{vir} for the virtual populations and the corresponding increments $\varepsilon(L, L_{vir})$ of the fitness measure $\mu(L)$ (7)

	Plots		
	meadow 1	meadow 2	felling 4
Submatrix L_{vir}	$\begin{bmatrix} a/294 & b/24 & c/25 & d/29 & 0 \\ 81/294 & 0 & 0 & 0 & 0 \\ e/294 & 0 & f/25 & g/29 & \frac{(h+1)}{10} \\ 63/294 & 0 & 4/25 & 0 & 0 \\ 8/294 & 0 & 0 & 0 & 0 \end{bmatrix}$	$\begin{bmatrix} a/218 & b/27 & c/13 & d/18 \\ 78/218 & 0 & 0 & 0 \\ e/218 & 0 & f/13 & \frac{g}{18} + \frac{h}{5} \\ 16/218 & 0 & 0 & 0 \end{bmatrix}$	$\begin{bmatrix} a/193 & b/37 & c/8 & d/11 & e/14 \\ 82/193 & 0 & 0 & 0 & 0 \\ f/193 & 0 & \frac{g}{8} + \frac{h}{8} & g/29 & \frac{(h+1)}{10} \\ 2/193 & 0 & 4/25 & 0 & 0 \\ 1/193 & 0 & 0 & 0 & 0 \end{bmatrix}$
$[\lambda_{1min}, \lambda_{1max}]$	[1.2595, 1.3192]	[1.5020, 1.5516]	[0.9051, 1.0476]
Increment of measure (7)	[0.0001, 0.0001]	[0.0400, 00400]	[0.0258, 0.0258]

modification consolidating them with the core gives the LCGs of *virtual* populations, and the corresponding reproductive-core submatrices L_{vir} are listed in Table 6. The $\lambda_{1min}(L_{vir})$ and $\lambda_{1max}(L_{vir})$ were calculated for the corresponding values of parameters a, b, ..., h from Table 4, as well as the increments $\varepsilon(L, L_{vir})$, which refine the measure $\mu(L)$ according to (7).

ACKNOWLEDGMENTS

This work was supported by the Russian Foundation for Basic Research, project no. 13-04-01836.

We are grateful to Prof. A.S. Komarov for valuable criticism that improved the quality of the manuscript.

REFERENCES

Akshentsev, E.V., et al., *Polivariantnost' razvitiya organizmov, populyatsii i soobshchestv: monografiya* (Polyvariant Development of Organisms, Populations, and Communities: Monograph), Voskresenskaya, O.L., Ed., Yoshkar-Ola: Mariisk. Gos. Univ., 2006.

Bashmakova, I.G., *Diofant i diofantovy uraveneniya* (Diophantus and Diophantine Equations), Moscow: LKI, 2007.

Bel'kov, V.P., Some regularities of development of living cover on logging sites, *Dokl. Akad. Nauk SSSR*, 1960, vol. 130, no. 6, pp. 1370–1373.

Caswell, H., *Matrix Population Models: Construction, Analysis, and Interpretation*, Sunderland, MA: Sinauer, 1989.

Caswell, H., *Matrix Population Models: Construction, Analysis, and Interpretation*, Sunderland, MA: Sinauer, 2001, 2nd ed.

Cushing, J.M. and Yicang, Z., The net reproductive value and stability in matrix population models, *Nat. Res. Model.*, 1994, vol. 8, pp. 297–333.

Diophantine equation. http://en.academic.ru/dic.nsf/enwiki/5320.

Ermakova, I.M., Sugorkina, N.S., Tarasenko, T.E., and Skvortsova, E.S., Influence of economic activities on the structure and harvest of the flood land meadow, Trudy mezhd. konf. po fitotsenologii i sistematike vysshikh rastenii, posvyashchennaya 100-letiyu so dnya rozhdeniya A.A. Uranova (Proc. Int. Conf. on Phytocenology and Systematics of Higher Plants Dedicated to the 100th Anniversary of A.A. Uranov), 2001, pp. 60–62.

Gantmakher, F.R., *Teoriya matrits* (The Theory of Matrices), Moscow: Nauka, 1967.

Gyllenberg, M. and Service, R., Necessary and sufficient conditions for the existence of an optimisation principle in evolution, *J. Math. Biol.*, 2011, vol. 62, pp. 359–369.

Harary, F., Norman, R.Z., and Cartwright, D., *Structural Models: an Introduction to the Theory of Directed Graphs*, New York: Wiley, 1965.

Horn, R.A. and Johnson, C.R., *Matrix Analysis*, Cambridge: Cambridge Univ. Press, 1990.

Janczyk-Weglarska, J., An ex situ ecological experiment on the morphological and developmental variation of Calamagrostis epigeios (Poaceae), Fragm. Florist. *Geobot.*, 1997, vol. 42, no. 2, pp. 239–247.

Li, C.-K. and Schneider, H., Application of Perron–Frobenius theory to population dynamics, *J. Math. Biol.*, 2002, vol. 44, pp. 450–462.

Logofet, D.O., *Matrices and Graphs: Stability Problems in Mathematical Ecology*, Boca Raton, FL: CRC Press, 1993.

Logofet, D.O., Three sources and three constituents of the formalism for a population with discrete age and stage structures, *Mat. Model.*, 2002, vol. 14, no. 12, pp. 11–22.

Logofet, D.O., Convexity in projection matrices: projection to a calibration problem, *Ecol. Model.*, 2008, vol. 216, no. 2, pp. 217–228.

Logofet, D.O., Svirezhev's substitution principle and matrix models for dynamics of populations with complex structures, *Zh. Obshch. Biol.*, 2010, vol. 71, no. 1, pp. 30–40.

Logofet, D.O., Projection matrices in variable environments: m1 in theory and practice, *Ecol. Model.*, 2013a, vol. 251, pp. 307–311.

Logofet, D.O., Calamagrostis model revisited: matrix calibration as a constraint maximization problem, *Ecol. Model.*, 2013b, vol. 254, pp. 71–79.

Logofet, D.O., Complexity in matrix population models: polyvariant ontogeny and reproductive uncertainty, *Ecol. Complexity*, 2013c, vol. 15: 43–51.

Logofet, D.O., Projection matrices revisited: a potential growth indicator and the merit of indication, *J. Math. Sci.*, 2013d, vol. 193, no. 5, pp. 671–686.

Logofet, D.O. and Belova, I.N., Nonnegative matrices as a tool to model population dynamics: classical models and contemporary expansions, *J. Math. Sci.*, 2008, vol. 155, no. 6, pp. 894–907.

Logofet, D.O., Ulanova, N.G., and Belova, I.N., Two paradigms in mathematical population biology: an attempt at synthesis, *Biol. Bull. Rev.*, 2012, vol. 2, no. 1, pp. 89–104.

Logofet, D.O., Ulanova, N.G., and Belova, I.N. Adaptation on the ground and beneath: does the local population maximize its λ_1? *Ecol. Complexity*, 2014, vol. 20, pp. 176–184.

Logofet, D.O., Ulanova, N.G., Klochkova, I.N., and Demidova, A.N, Structure and dynamics of a clonal plant population: classical model results in a non-classic formulation, *Ecol. Model.*, 2006, vol. 192, pp. 95–106.

MathWorks, 2012. http://www.mathworks.com/help/toolbox/optim/ug/fmincon.html.

Metz, J.A.J., Mylius, S.D., and Diekmann, O., When does evolution optimize? *Evol. Ecol. Res.*, 2008a, vol. 10, pp. 629–654.

Metz, J.A.J., Mylius, S.D., and Diekmann, O., Even in the odd cases when evolution optimizes, unrelated population dynamical details may shine through in the ESS, *Evol. Ecol. Res.*, 2008b, vol. 10, pp. 655–666.

Onipchenko, V.G. and Komarov, A.S., Life duration and dynamics of the high-altitude plant populations: analysis of three alpine species of the Northwestern Caucasus, *Zh. Obshch. Biol.*, 1997, vol. 58, no. 6, pp. 64–75.

Pathikonda, S., Ackleh, A.S., Hasenstein, K.H., and Mopper, S., Invasion, disturbance, and competition: modeling the fate of coastal plant populations, *Conserv. Biol.*, 2009, vol. 23, pp. 164–173.

Patrabolova, I.G., Biology of the bushgrass related to recovery of pine plantations in Buzulukskiy pine forest, Extended Abstract of Cand. Sci. (Biol.) Dissertation, Moscow: Moscow State Pedagog. Inst., 1953.

Prach, K. and Pyšek, P., How do species dominating in succession differ from others? *J. Veg. Sci.*, 1999, vol. 10, no. 3, pp. 383–392.

Protasov, V.Yu. and Logofet, D.O., Rank-one corrections of nonnegative matrices, with an application to matrix population models, *SIAM J. Matrix Anal. Appl.*, 2014, vol. 35, no. 2, pp. 749–764.

Rabotnov, T.S., *Fitotsenologiya* (Phytocenology), Moscow: Mosk. Gos. Univ., 1978.

Sabinin, D.A., *Fiziologiya razvitiya rastenii* (Physiology of the Plant Development), Moscow: Akad. Nauk SSSR, 1963.

Serebryakova, T.I., *Morfogenez pobegov i evolyutsiya zhiznennykh form zlakov* (Morphogenesis of Shoots and Evolution of the Life Forms of Cereals), Moscow: Nauka, 1971.

Shea, K. and Kelly, D., Estimating biocontrol agent impact with matrix models: Carduus nutans in New Zealand, *Ecol. Appl.*, 1998, vol. 8, no. 3, pp. 824–832.

Ulanova, N.G., Calamagrostis epigeios, in Biologicheskaya flora Moskovskoi oblasti (Biological Flora of Moscow Region), Moscow: *Argus*, 1995, vol. 10, pp. 4–19.

Ulanova, N.G., Population dynamics of bushgrass after demutation of vegetation on the logging sites, in *Populyatsii i soobshchestva rastenii: ekologiya, bioraznoobrazie, monitoring* (The Plant Populations and Communities: Ecology, Biodiversity, and Monitoring), Kostroma: Kostrom. Gos. Pedagog. Univ., 1996, vol. 2, pp. 24–25.

Ulanova, N.G., Plant age stages during succession in woodland clearings in Central Russia, in *Vegetation Science in Retrospective and Perspective*, Uppsala: Opulus, 2000, pp. 80–83.

Ulanova, N.G., Dynamics of vegetation recovery on the solid logging sites and mass windfalls in the spruce forests of southern taiga in European Russia, Extended Abstract of Doctoral (Biol.) Dissertation, Moscow: Mosk. Gos. Univ., 2006.

Ulanova, N.G., Belova, I.N., and Logofet, D.O., Competition among populations with discrete structure: the dynamics of populations of reed and birch growing together, *Zh. Obshch. Biol.*, 2008, vol. 69, no. 6, pp. 478–494.

Ulanova, N.G. and Demidova, A.N., Population biology of the purple small-reed (Calamagrostis canescens (Web.) Roth) on the logging sites of southern spruce taiga, Byull. Mosk. O-va. Ispyt. Prir., *Otd. Biol.*, 2001, vol. 106, no. 5, pp. 51–58.

Ulanova, N.G., Demidova, A.N., Logofet, D.O., and Klochkova, I.N., Structure and dynamics of Calamagrostis canescens coenopopulation: a model approach, *Zh. Obshch. Biol.*, 2002, vol. 63, no. 6, pp. 509–521.

Ulanova, N.G., Klochkova, I.N., and Demidova, A.N., Modeling of the population dynamics of Calamagrostis epigeios (L.) Roth during overgrowing of the logging site of complex spruce forest, Sib. Bot. Vestn., 2007, vol. 2, no. 2, pp. 91–96. http://journal.csbg.ru.

Uranov, A.A., Ontogenesis and age composition of the populations, in *Ontogenez i vozrastnoi sostav tsvetkovykh rastenii* (Ontogenesis and Age Composition of the Population of Flowering Plants), Moscow: Nauka, 1967, pp. 3–9.

Uranov, A.A., Age diversity of the plant populations as the function of time and energy wave processes, Biol. Nauki, 1975, no. 2, pp. 7–34.

Weppler, T., Stoll, P., and Stocklin, J., The relative importance of sexual and clonal reproduction for population growth in the long-lived alpine plant Geum reptans, *J. Ecol.*, 2006, vol. 94, pp. 869–879.

Werner, P.A. and Caswell, H., Population growth rates and age versus stage distribution models for teasel (Dipsacus sylvestris Huds), *Ecology*, 1977, vol. 58, pp. 1103–1111.

Zhukova, L.A., Polyvariance of the meadow plants, in *Zhiznennye formy v ekologii i sistematike rastenii* (Life Forms in Ecology and Plant Systematics), Moscow: Mosk. Gos. Pedagog. Inst., 1986, pp. 104–114.

Zhukova, L.A., *Populyatsionnaya zhizn' lugovykh rastenii* (Population Life of the Meadow Plants), Yoshkar-Ola: Lanar, 1995.

Zhukova, L.A. and Komarov, A.S., Polyvariance of ontogenesis and dynamics of plant populations, *Zh. Obshch. Biol.*, 1990, vol. 51, no. 4, pp. 450–461.

Zaugol'nova, L.B., Zhukova, L.A., Komarov, A.S., and Smirnova, O.V., *Tsenopopulyatsii rastenii (ocherki populyatsionnoi biologii)* (The Plant Cenopopulations: Reviews on Population Biology), Moscow: Nauka, 1988.

Translated by G. Chirikova